Acta Cryst. (1976). B32, 878

Crystal Structure of a Second Phase of 1-Ethyl-1-methyl-4-phenylpiperidinium Perchlorate. Analysis of the Intramolecular Geometry and Perchlorate Motion by means of Potential Energy Calculations

BY W. FEDELI AND F. MAZZA

Laboratorio di Strutturistica Chimica 'Giordano Giacomello' CNR, C.P. N° 10, 00016 Monterotondo Stazione, Roma, Italy

AND E. GIGLIO, C. QUAGLIATA AND N. SCARCELLI

Istituto di Chimica-fisica, Università di Roma, 00185 Roma, Italy

(*Received* 11 *August* 1975; *accepted* 14 *August* 1975)

A second monoclinic phase (SMP) of 1-ethyl-1-methyl-4-phenylpiperidinium perchlorate ($C_{14}H_{22}NClO_4$, EMPPP) crystallizes in space group $P2_1$, with $a=6{\cdot}78$ (2), $b=8{\cdot}27$ (2), $c=14{\cdot}56$ (4) Å, $\beta=100{\cdot}5°$ (2), $Z=2$. The structure was determined from 1239 X-ray intensities, measured by the equi-inclination Weissenberg technique. Refinement was by least-squares methods to a final R of 0·12. The perchlorate ion executes a large rotational motion around a Cl–O bond. Fourier difference synthesis and potential energy calculations support this model. The intramolecular potential energy was computed in order to clarify some unusual bond angles displayed by the 1-ethyl-1-methyl-4-phenylpiperidinium cation (PPC) in both monoclinic phases. The analysis of the van der Waals interactions indicates that some intramolecular contacts are responsible for the widening of some angles.

Introduction

The structure of a first monoclinic phase (FMP) of EMPPP was solved by Fedeli, Mazza & Vaciago (1970) in order to throw light on the quaternization mechanism of a substituted piperidine (Jones, Katritzky, Richards & Wyatt, 1970; Jones, Katritzky & Mente, 1970).

PPC and its atomic numbering are shown in Fig. 1. In the following, the H atoms have the same numbering as the C atoms to which they are bonded, a prime or a double prime indicating an axial or equatorial H atom respectively.

Table 1. *Crystal data (room temperature) of the two monoclinic phases of EMPPP*

	FMP	SMP
λ (Å)	1·5418	1·5418
a (Å)	6·19 (2)	6·78 (2)
b (Å)	7·97 (2)	8·27 (2)
c (Å)	32·32 (9)	14·56 (4)
β (°)	104·0 (2)	100·5 (2)
Z	4	2
Systematic absences	$h0l$: $l\neq 2n$ $0k0$: $k\neq 2n$	$0k0$: $k\neq 2n$
Space group	$P2_1/c$	$P2_1$
D_c (g cm^{-3})	$1{\cdot}30_4$	$1{\cdot}25_6$
M.W. (a.m.u.)	303·8	303·8
μ(Cu $K\alpha$) (cm^{-1})	23·0	22·2

Only two crystals of SMP, suitable for X-ray intensity collection, were found in the same crystallization bath as FMP, thus preventing density measurements. The crystal data of these two phases are reported in Table 1. The following reasons prompted us to undertake the determination of the structure of SMP:

(1) The density of SMP is notably lower than that of FMP, which itself has large atomic thermal parameters. Therefore, some disorder could be expected in SMP, thus allowing us to verify the ability of potential energy calculations to supply adequate models to describe a disordered structure.

(2) The C(3)–C(4)–C(10) and C(4)–C(10)–C(11) angles of PPC (see Fig. 1) in FMP are both wider (116·5 and 123·2° respectively) than the usual values corresponding to tetrahedral and trigonal hybridization. Although it is impossible to gain detailed information about the molecular geometry, owing to the low accuracy of the structure determination, the observed conformation of PPC seems to indicate the reliability of these values. In fact, C(3), C(11), H′(3) and H(11) form some short contacts if standard bond angles are assumed. Hence the study of SMP was considered of interest to ascertain if there were analogies between the two phases in relation to the conformation and geometry of PPC, and if we could predict the experimental conformations by computing the PPC intramolecular energy map.

(3) PPC of FMP is the isomer formed by preferential axial attack in the reaction of 1-ethyl-4-phenylpiperidine with methyl iodide. SMP might be due to the formation of a small amount of the other isomer.

Experimental

Prismatic crystals of SMP were obtained with those of FMP by slow evaporation of an aqueous solution

at room temperature. The intensities of 1239 independent reflexions, belonging to the *h*0*l*–*h*4*l* and 0*kl*–5*kl* layers and corresponding to 63% of the whole sphere of reflexion, were collected on multiple-film equi-inclination Weissenberg photographs with Cu $K\alpha$ radiation. The intensities, visually estimated, were corrected for Lorentz, polarization and change of spot shape on upper layers. No absorption correction was applied. The observed structure amplitudes were placed on a common scale by the method of Hamilton, Rollett & Sparks (1965).

Structure determination and refinement

The Cl atoms were located from a Patterson function. Iterative structure factor and Fourier synthesis calculations allowed us to assign atomic coordinates to all the non-hydrogen atoms with the exception of the O atoms. Five maxima of the electron density were found around the Cl atom at distances consistent with the usual Cl–O length. A difference synthesis showed four of these maxima lying on a continuous toroidal region. This suggested that the perchlorate ion was partially or completely rotating around Cl–O(1), O(1) being the atom corresponding to the only maximum located outside the toroidal region. Furthermore, only O(1) forms suitable O–Cl–O angles.

However, before assuming this reasonable model, all the possible perchlorate groups were tested by taking in turn four of the five maxima as O atoms. Moreover, all possible structures with two equally weighted perchlorate ions, having the Cl atoms coinciding, were tried with appropriate occupancy factors. No satisfactory results were achieved. The least-squares refinements were carried out with the programs of Domenicano, Spagna & Vaciago (1969). Scattering factors for C, N, O, and Cl were from Cromer & Mann (1968) and for H from Hanson, Herman, Lea & Skillman (1964).

At the same time the rotational freedom of the perchlorate group was checked both in FMP and SMP by potential energy calculations, moving the ClO_4^- ions and keeping the PPC's fixed. The coefficients of the van der Waals potentials in the generalized form:

$$V(r)=a\exp(-br)/r^d-cr^{-6}$$

are listed in Table 2 (Coiro, Giglio & Quagliata, 1972, and references quoted therein). The electrostatic energy was computed from the simple Coulomb law:

$$V(r_{ij})=Z_iZ_j/r_{ij}D,$$

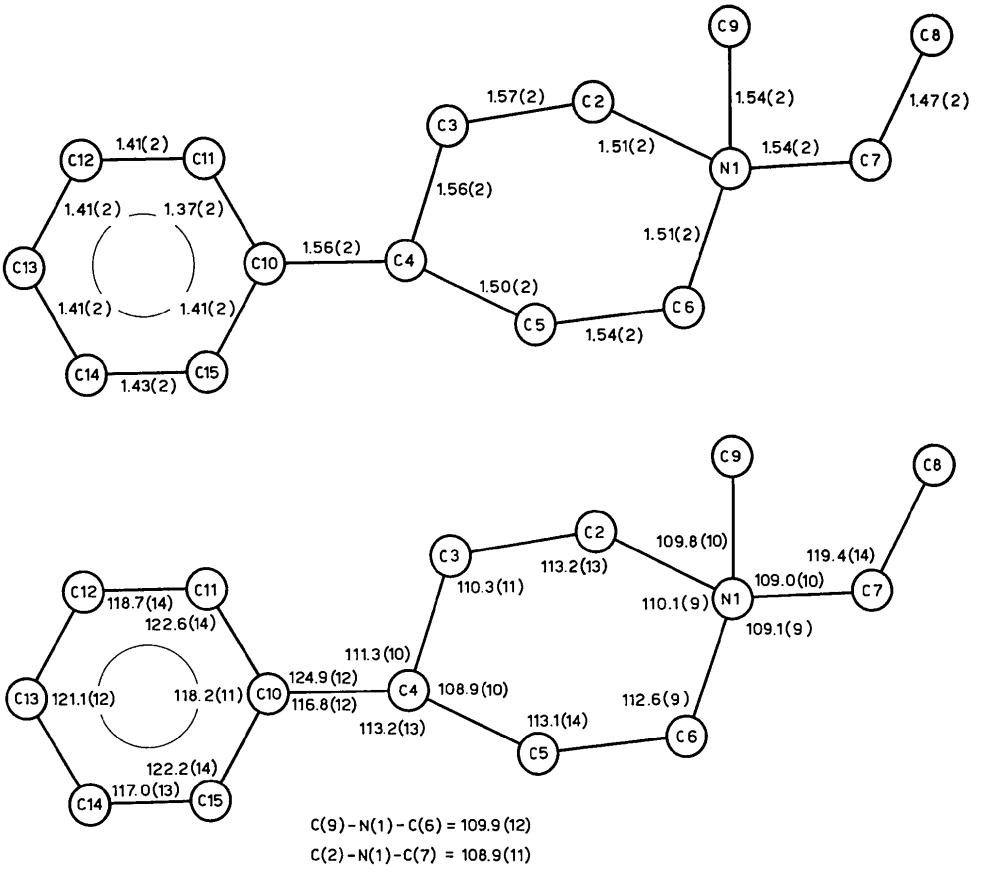

Fig. 1. Atomic numbering, bond lengths (Å) and angles (°) of PPC in SMP. The estimated standard deviations are given in parentheses.

Table 2. *The coefficients of the van der Waals potentials*

The energy is in kcal per atom pair if the interatomic distance is in Å.

Interaction	a ($\times 10^{-3}$)	b	c	d
H–H	6·6	4·080	49·2	0
H–C	44·8	2·040	125·0	6
H–N	52·1	2·040	132·0	6
H–O	42·0	2·040	132·7	6
H–CH_3	49·1	3·705	380·5	0
H–Cl	40·5	3·851	265·2	0
C–C	301·2	0·000	327·2	12
C–N	340·0	0·000	340·0	12
C–O	278·7	0·000	342·3	12
C–CH_3	291·1	1·665	981·1	6
C–Cl	255·4	1·811	684·0	6
N–N	387·0	0·000	354·0	12
N–O	316·2	0·000	356·0	12
N–CH_3	325·9	1·665	1020·5	6
N–Cl	288·6	1·811	711·5	6
O–O	259·0	0·000	358·5	12
O–CH_3	272·7	1·665	1026·3	6
O–Cl	239·2	1·811	715·5	6
CH_3–CH_3	273·9	3·329	2942·0	0
CH_3–Cl	251·6	3·475	2051·1	0
Cl–Cl	220·8	3·621	1430·0	0

where r_{ij} is the distance between the charged atoms i and j, Z_i and Z_j the atomic charge and D the dielectric constant. The atomic charges of the N and O atoms were assumed to be +1 and −0·25 respectively. The dielectric constant was taken as unity since only the interactions between one asymmetric unit and the first shell of EMPPP's were considered, applying the same strategy as in the analysis of sodium oxalate and formate, potassium methoxide, potassium, rubidium and caesium acetylenediolate (Capaccio, Giacomello & Giglio, 1971), sodium tetrazolate monohydrate and sodium, potassium and rubidium azides (Dosi, Giglio, Pavel & Quagliata, 1973). The atomic coordinates of the C and N atoms were the experimental ones, while those of the H atoms were generated at the expected positions as follows: (*a*) the C–H length is 1·08 Å; (*b*) in the phenyl ring every H atom lies on the bisector of the C–C–C angle, the central C being bound to the H atom; (*c*) in the piperidinium ring and in the CH_2 of the ethyl group every H atom forms two H–C–C (or one H–C–C and one H–C–N) angles of 109·5°. The methyl group was treated as one atom.

Because the ClO_4^- ion has large thermal motion in FMP and some orientational disorder in SMP, a regular tetrahedral geometry with Cl–O distances of 1·44 Å was chosen for this group. The energy minima search depends on three rotation angles of the ClO_4^- group and was carried out in FMP by taking into account 18 asymmetric units in addition to the central one. The deepest minimum satisfactorily corresponds to the observed structure. Thus the suggestion that the unusual thermal motion of the O atoms conceals orientational disorder can be reasonably ruled out. The potential energy calculations were performed in SMP by considering in the last computation 52 asymmetric units besides the central one to be sure that the long-range electrostatic contributions would not change the minima location. Only one very large and broad minimum was found in the analysis of the energy. The coordinates of the O atoms were determined for some sample points located in the minimum of the energy map. These atomic coordinates fitted the O(1) maximum and the toroidal zone of the difference synthesis, so that the model of the perchlorate group rotating around Cl–O(1) was further supported.

At this stage it was decided to evaluate qualitatively the potential energy in the crystal of SMP as a function of the rotation angle ψ around Cl–O(1), preserving the conditions mentioned before. The starting position, $\psi = 0°$, gave one O atom, different from O(1), with fractional coordinates $x = 0{\cdot}401$, $y = 0{\cdot}338$, $z = 0{\cdot}199$. The coordinates of Cl coincided with those derived from the last Fourier synthesis, before starting the refinement. O(1) was placed on the experimental Cl–O(1) bond at 1·44 Å from Cl. The rotation was taken as positive if, looking along Cl–O(1), the O atoms are moved clockwise.

After the structure was refined the Cl and O(1) atomic coordinates changed very little with respect to those used in this analysis and, therefore, the curves of Fig. 2 are those computed anew by employing the final atomic coordinates. Curve (*a*) shows the contributions of the van der Waals and Coulombic energies, which give rise to a potential well in the range 60–120°, the minimum being at 95°. The corresponding coordinates of the oscillating O atoms do not all fit either three peaks of the difference synthesis or the positional parameters of three O atoms obtained after refinement was complete. The shape of the minimum seems to indicate that the ClO_4^- ion undergoes a torsional oscillation about the Cl–O(1) vector around 95°, the moving O atoms always lying inside the toroidal region.

From the inspection of the H···O contacts it was inferred that there are some distances, shorter than the sum of the van der Waals radii of H and O (~2·6 Å), involving H″(6) and H(11) of the asymmetric units at $(1-x, \frac{1}{2}+y, 1-z)$ and $(-x, \frac{1}{2}+y, 1-z)$ respectively and one oscillating O atom of the ClO_4^- group at (x,y,z).

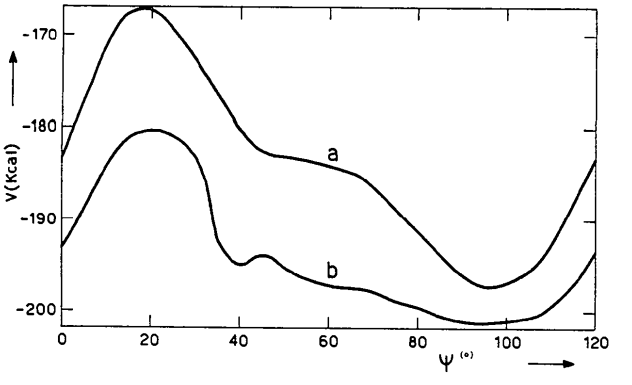

Fig. 2. Potential energy *vs.* the rotation angle ψ around Cl–O(1). Curve (*a*): van der Waals and Coulombic energy; curve (*b*): as (*a*) plus hydrogen-bonding energy.

These distances can be as short as 2·15 Å, thus not precluding the formation of C–H···O–Cl weak hydrogen bonds. Such an occurrence was taken into account by introducing in the energy calculations the potential proposed by Stockmayer (1941) for two polar gas molecules, successfully employed in crystal packing analyses (Giglio, 1969; Giacomello & Giglio, 1970; Coiro, Giacomello & Giglio, 1971; Dosi *et al.*, 1973). The potential energy is expressed by

$$V(r,\theta_a,\theta_b,\varphi)=4\epsilon[(\sigma/r)^{12}-(\sigma/r)^6]$$
$$-\mu_a\mu_b r^{-3}(2\cos\theta_a\cos\theta_b-\sin\theta_a\sin\theta_b\cos\varphi).$$

The Lennard–Jones term refers to the dispersion and the repulsive energy of the H···O interaction. The remaining term gives the electrostatic energy between two point dipoles centred on H and O atoms and oriented along C–H and Cl–O. The values of the parameters $\epsilon=0{\cdot}0047$ kcal, $\sigma=2{\cdot}83$ Å and $\mu_a\mu_b=18{\cdot}27$ kcal Å^3 were evaluated (Giglio, 1969) by putting $V=-3{\cdot}5$ kcal and $\partial V/\partial r=0$ when the H···O distance, r, is equal to 2 Å and the C, H, O and Cl atoms are collinear, since in the cases of interest the angle H···O–Cl was mainly within the range 150–175°. A cut-off distance of 2·45 Å was assumed in the calculations. Although curve (*b*) of Fig. 2, computed by adding the hydrogen-bonding energy to the van der Waals and Coulombic ones, displays the same behaviour as curve (*a*), it is more flattened with a less prominent energy barrier. Then the model with the ClO_4^- ion experiencing a large torsional oscillation, for example in the range 55–115°, is still more convincing, owing to the small difference between the energies at 55° (−196·7 kcal) and 95° (−201·4 kcal) in spite of our hard van der Waals potentials which have steep energy gradients.

Hence the refinement started from a trial structure consisting of a PPC, Cl and O(1) atoms, determined from electron density maps, and four O atoms with occupancy factors of 0·75, placed in the toroidal region at nearly equal intervals. The Cl–O lengths were 1·44 Å and the O(1)–Cl–O angles 109·5°. The quantity minimized was $\sum w(|F_o|-|F_c|)^2$ where $w=(2{\cdot}2+|F_o|+0{\cdot}022|F_o|^2)^{-1}$. Refinement proceeded by isotropic and anisotropic block-diagonal least-squares methods keeping fixed, initially, the coordinates of the O atoms, which were subsequently refined with isotropic temperature factors. The H atoms, generated as above, except that those of the two methyl groups were in staggered conformation with respect to the bonds of N(1) and C(7), were included in the last cycles with an isotropic B of 5 Å^2. The refinement, carried out with the observed reflexions, was terminated at $R=0{\cdot}12$ and $R_w=0{\cdot}15$, the parameter shifts of the Cl, O(1) and PPC atoms being less than the estimated standard deviations. Other attempts to achieve better results by increasing the number of O atoms and by suitably lowering their occupancy factors in the toroidal zone

Table 3. *Final values of the fractional atomic coordinates* ($\times 10^4$) *of EMPPP with standard deviations in parentheses*

	x	*y*	*z*
O(1)	1220 (19)	3305 (19)	721 (9)
O(2)	4385 (29)	2689 (34)	1552 (14)
O(3)	856 (36)	2552 (47)	2259 (16)
O(4)	2416 (25)	936 (27)	1608 (11)
O(5)	2771 (32)	3819 (33)	2193 (15)
Cl	2243 (5)	2483*	1587 (2)
N(1)	2866 (11)	2317 (16)	8326 (6)
C(2)	1173 (22)	3500 (21)	8050 (11)
C(3)	−522 (19)	2846 (25)	7259 (11)
C(4)	376 (17)	2331 (22)	6391 (8)
C(5)	2027 (17)	1140 (22)	6693 (8)
C(6)	3676 (17)	1787 (21)	7475 (8)
C(7)	4554 (20)	3145 (21)	9018 (10)
C(8)	6364 (20)	2222 (27)	9410 (9)
C(9)	2117 (26)	837 (22)	8803 (10)
C(10)	−1284 (16)	1685 (20)	5592 (8)
C(11)	−2727 (19)	582 (23)	5707 (10)
C(12)	−4249 (20)	97 (22)	4968 (12)
C(13)	−4266 (21)	749 (23)	4070 (10)
C(14)	−2749 (24)	1820 (22)	3902 (9)
C(15)	−1248 (20)	2258 (22)	4686 (9)

* This coordinate was kept fixed during the refinement.

Table 4. *Thermal parameters* ($\times 10^4$) *for EMPPP with standard deviations in parentheses*

The form of the temperature factor is $\exp[-(b_{11}h^2+b_{12}hk+b_{13}hl+b_{22}k^2+b_{23}kl+b_{33}l^2)]$.

B values for O atoms: O(1) 10·9 (3), O(2) 13·1 (6), O(3) 16·4 (8), O(4) 11·7 (5), O(5) 14·7 (6).

	b_{11}	b_{22}	b_{33}	b_{12}	b_{13}	b_{23}
Cl	383 (7)	202 (4)	76 (1)	5 (13)	35 (5)	−19 (6)
N(1)	227 (19)	209 (18)	71 (5)	4 (34)	68 (15)	−37 (18)
C(2)	437 (41)	302 (32)	105 (10)	273 (64)	−35 (34)	−117 (31)
C(3)	290 (32)	440 (53)	108 (10)	242 (70)	−13 (29)	−153 (40)
C(4)	283 (29)	291 (28)	79 (6)	−32 (57)	14 (22)	36 (29)
C(5)	289 (30)	388 (39)	66 (6)	139 (56)	76 (23)	−43 (27)
C(6)	254 (27)	358 (31)	67 (6)	122 (52)	105 (21)	−4 (25)
C(7)	382 (37)	295 (31)	92 (9)	−57 (58)	8 (29)	−60 (28)
C(8)	361 (36)	418 (48)	82 (7)	36 (75)	−52 (25)	−22 (36)
C(9)	598 (58)	290 (31)	92 (9)	−348 (74)	112 (37)	−3 (28)
C(10)	256 (27)	304 (26)	76 (7)	1 (49)	59 (22)	−2 (26)
C(11)	337 (37)	349(34)	85 (8)	−92 (64)	43 (27)	−20 (31)
C(12)	303 (34)	301 (32)	141 (12)	10 (59)	183 (35)	−72 (35)
C(13)	373 (40)	334 (35)	88 (8)	16 (65)	−25 (28)	−62 (31)
C(14)	569 (49)	280 (29)	75 (8)	−131 (68)	−58 (31)	27 (28)
C(15)	416 (39)	299 (34)	86 (7)	−188 (65)	50 (27)	39 (29)

were unsuccessful. The final atomic coordinates and thermal parameters are reported in Tables 3 and 4. A list of observed and calculated structure factors is given in Table 5. The crystal packing is shown in Fig. 3.

Potential energy calculations for PPC

The C(3)–C(4)–C(10)–C(11) torsion angle deserves some attention both in FMP and SMP, since the ob-

Table 5. *Observed and calculated structure factors* ($\times 10$) *for EMPPP*

served values, according to the convention of Klyne & Prelog (1960), which will be used later, are 34·7 and 47·4° instead of the most favourable 60°. These experimental values correspond to short H'(3)···H(11) contacts, if a regular geometry is assumed for PPC, and are reported in Fig. 4, where φ represents the H(4)–C(4)–C(10)–C(15) dihedral angle. These contacts can be improved by opening the C(3)–C(4)–C(10) and C(4)–C(10)–C(11) angles, as occurs in both the observed structures (see Fig. 4). A similar situation was found in 1-benzyl-1-ethyl- and 1-benzyl-1-isopropyl-4-phenylpiperidinium chlorides (Carruthers, Fedeli, Mazza & Vaciago, 1973). In fact, the C(3)–C(4)–C(10), C(4)–C(10)–C(11), C(3)–C(4)–C(10) and C(4)–C(10)–C(11) torsion and bond angles are, respectively, 22·4, 113·4 and 125·1° for the ethyl and 49·9, 114·2 and 123·0° for the isopropyl derivative.

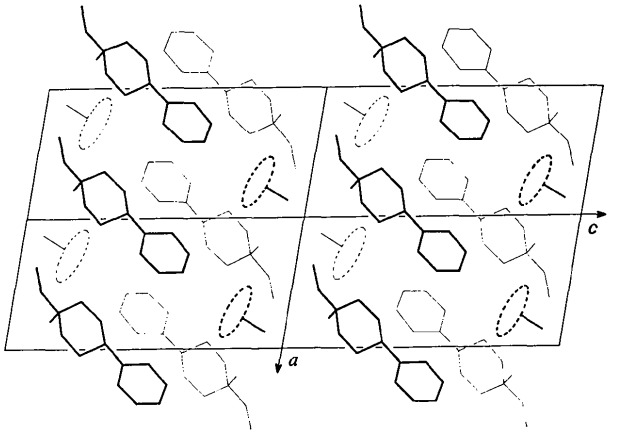

Fig. 3. Crystal packing of EMPPP viewed along b. The dotted lines represent the oscillating O atoms.

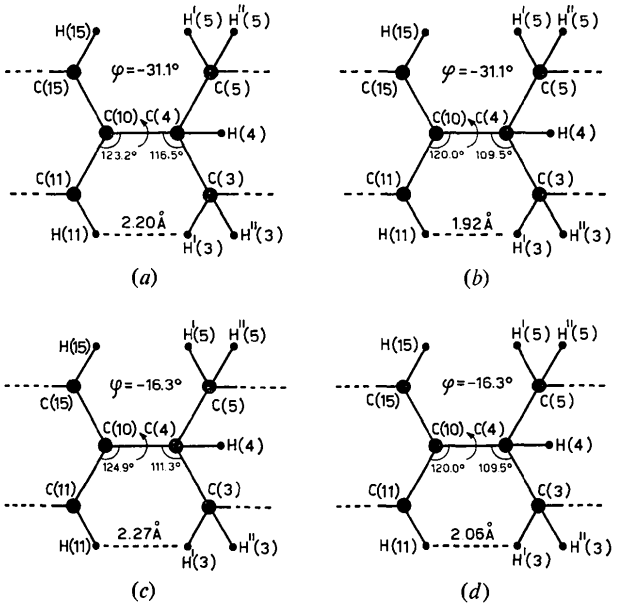

Fig. 4. Some relevant bond and torsion angles and H'(3)···H(11) contact for PPC. (*a*) and (*c*): actual geometry in FMP and SMP; (*b*) and (*d*): standard models with the same φ as in (*a*) and (*c*).

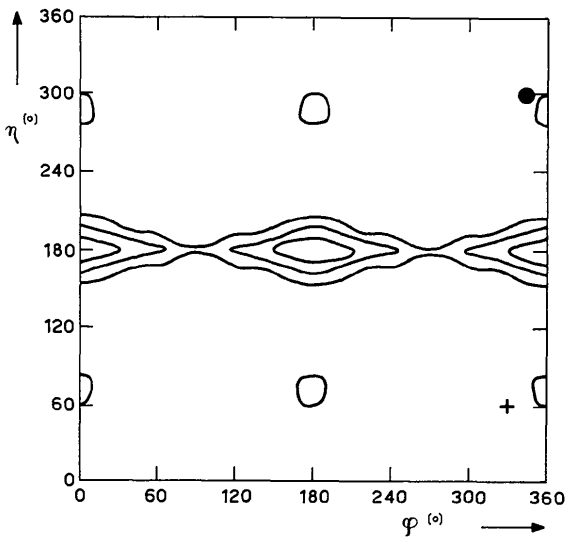

Fig. 5. Van der Waals energy as a function of φ and η for a standard model of PPC. Contour lines are drawn at 10·5, 12·0 and 13·5 kcal. The cross and the black dot indicate the dihedral angles found in FMP and SMP respectively.

In order to verify the PPC conformational stability in FMP and SMP, intramolecular potential energy calculations were performed as a function of the rotation angles about N(1)–C(7) and C(4)–C(10) and with angular increments of 10°. Firstly the van der Waals energy was computed for a standard model with the potentials of Table 2 and the following lengths and angles: C–H = 1·08, C–C = 1·53, C–N = 1·51 Å; C–C–C and H–C–C = 120° (in the phenyl ring); C–C–C = 112·0°; C(2)–N(1)–C(6) = 111·6°; C(2)–N(1)–C(9) = C(6)–N(1)–C(9) = 109·5°; C(9)–N(1)–C(7) = 107·2°; N(1)–C(7)–C(8) = 115·0°; H–C–C and H–C–N = 109·5° (in the piperidinium ring).

The corresponding map is shown in Fig. 5, where η is the C(8)–C(7)–N(1)–C(9) torsion angle and φ is defined as before. The deepest minimum, as expected, is at $\varphi = 0°$ (or 180°) and $\eta = 180°$, while the actual conformations have $\varphi = -31·1°$, $\eta = 59·3°$ in FMP and $\varphi = -16·3°$, $\eta = -58·7°$ in SMP (see Fig. 5). The respective points on the map have energy values at least 5 kcal higher than that of the absolute minimum.

Subsequently the same calculation was made with the experimental geometry of PPC derived from FMP (Fig. 6) and SMP (Fig. 7). Of course, the symmetry in Fig. 5 is lacking in Figs. 6 and 7. The minima at $\eta = 70°$ and $-70°$ are lowered with respect to those of Fig. 5 and their values approach those of $\eta = 180°$. The enlargement of N(1)–C(7)–C(8) in SMP, 119·4° against 115·5° in FMP, is mainly responsible for the general lowering of the energy map of Fig. 7 compared with

that of Fig. 6. Moreover the minima of FMP at $\eta = -70°$ [C(8) staggered with respect to C(6) and C(9)] are higher than those at $\eta = 70°$ [C(8) staggered with respect to C(2) and C(9)], since C(6)–N(1)–C(7) is less than C(2)–N(1)–C(7) (106·9 and 110·1° respectively). The local minima at $\varphi = -30°$ and $\eta = 70°$ of FMP and at $\varphi = -10°$ and $\eta = -70°$ of SMP satisfactorily agree with the above mentioned actual values. Thus the molecular geometries of PPC, obtained from the determination of crystal structures with low accuracy, seem to be supported by the results of the potential energy calculations.

Discussion

PPC of SMP is the same isomer as found in FMP. The intramolecular distances and angles are summarized in Fig. 1. The rather large standard deviations and the high final R may be ascribed to the torsional oscillation of the ClO_4^- ion and to the lack of absorption corrections. The average C–C and C–N distances in the phenyl and chair-shaped piperidinium moieties are 1·41, 1·53 and 1·52 Å respectively. The average bond angles in the phenyl and piperidinium rings are 120·0 and 111·4°. All these values are in fair agreement with those of FMP, which are, in the same order, 1·38, 1·53, 1·52 Å, 120·0 and 111·3°. The phenyl ring is planar, the greatest deviation from the least-squares plane $0{\cdot}6157X - 0{\cdot}7649Y - 0{\cdot}2982Z + 4{\cdot}0001 = 0$ being 0·03 Å. The dihedral angles of the piperidinium ring vary, in magnitude, in the range 52–58° in FMP and 53–57° in SMP. The torsion angles C(2)–N(1)–C(7)–C(8) and C(3)–C(4)–C(10)–C(15) are −62·3 and −150·2° in FMP and −178·6 and −134·3° in SMP. Therefore C(2) and C(8) are in *gauche* and *trans* conformations in FMP and SMP with η of about $\pm 60°$ instead of the most favourable value of 180°. Really the energy difference is mainly due to the hardness of the $CH_3 \cdots CH_3$ potential used, since the contacts at $\eta = \pm 60°$, which arise by introducing C and H atoms, are satisfactory. On the other hand the phenyl ring approaches in SMP the φ value characterizing the global minimum, thus decreasing the PPC energy compared with that of FMP.

Most of the bond distances and bond angles involving the Cl and O atoms are, obviously, meaningless but are listed in Table 6. The Cl–O lengths agree with the standard, except that involving O(4). The positional standard deviations and the isotropic temperature factor of O(1) are the best among the O atoms and comparable with those of the C atoms. In addition the bond angles of O(1) show fair agreement with the regular tetrahedral value, while O(2), O(5), O(3), O(4) follow one another forming an average bond angle with Cl of 84°. These results support the model of the oscillating ClO_4^- ion. Furthermore, it is reasonable to suppose that approximately two O atoms oscillate about $\pm 30°$ around the maxima of the difference synthesis corresponding to O(2) and O(4), while a third oscillates around a point in the middle of the O(3)–O(5) arc. In fact, this last oscillation lies in the minimum energy range 55–115° of curve (*b*) of Fig. 2.

Table 6. *Bond distances* (Å) *and bond angles* (°) *of the* Cl *and* O *atoms*

Cl–O(1)	1·49	O(1)–Cl–O(2)	103	O(2)–Cl–O(4)	92
Cl–O(2)	1·47	O(1)–Cl–O(3)	107	O(2)–Cl–O(5)	78
Cl–O(3)	1·48	O(1)–Cl–O(4)	120	O(3)–Cl–O(4)	95
Cl–O(4)	1·28	O(1)–Cl–O(5)	101	O(3)–Cl–O(5)	71
Cl–O(5)	1·42	O(2)–Cl–O(3)	140	O(4)–Cl–O(5)	139

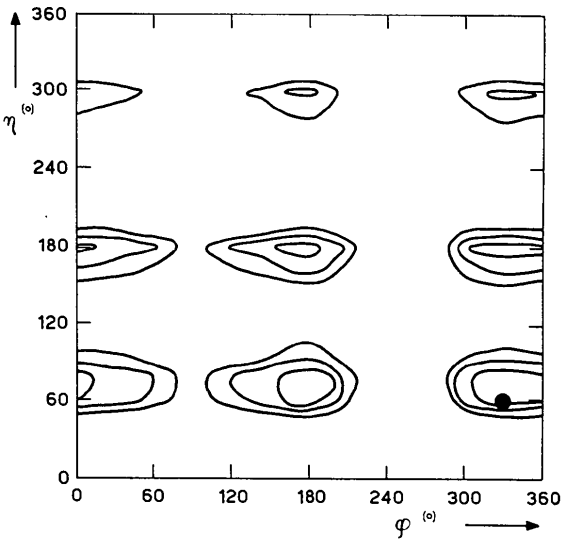

Fig. 6. Van der Waals energy as a function of φ and η for PPC of FMP. Contour lines are drawn at 10·5, 12·0 and 13·5 kcal. The black dot indicates the actual dihedral angles found in FMP.

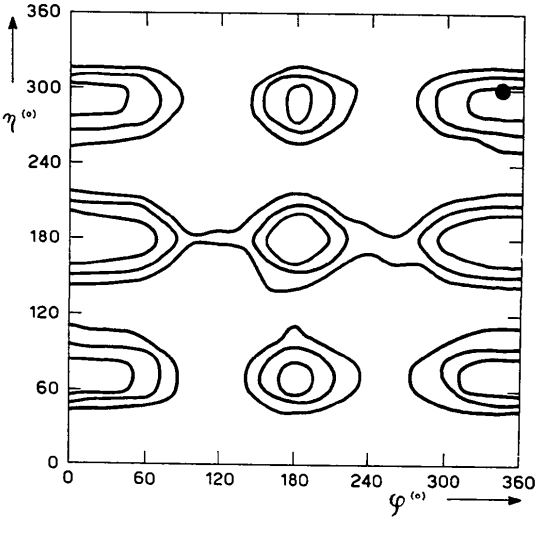

Fig. 7. Van der Waals energy as a function of φ and η for PPC of SMP. Contour lines are drawn at 8·5, 10·0 and 11·5 kcal. The black dot indicates the actual dihedral angles found in SMP.

A schematic drawing of the crystal packing is shown in Fig. 3. The molecules are tied together chiefly by electrostatic, van der Waals and, possibly, very weak hydrogen-bonding forces. No π–π interactions occur between two phenyl rings, adjacent along **a**, because the angle between their least-squares planes is 80°. Omitting the O atoms of the toroidal region, no short van der Waals contacts are present. The structure consists of screw-related layers normal to **b**, two adjacent layers being shifted about **c**/5 and **c**/3 with respect to the PPC and ClO_4^- ions. The molecular packing is very similar in FMP, where the two distinct layers are composed of asymmetric units at (x,y,z) and $(x,\frac{1}{2}-y,\frac{1}{2}+z)$ for the first and at $(\bar{x},\bar{y},\bar{z})$ and $(\bar{x},\frac{1}{2}+y,\frac{1}{2}-z)$ for the second. The approximate halving of **c** in SMP corresponds to the loss of the glide plane present in FMP, so that the glide symmetry is replaced by a translation.

We thank Professor A. R. Katritzky for supplying the compound and Mr A. Amorese for technical assistance.

E.G., C.Q. and N.S. acknowledge the financial support of the Consiglio Nazionale delle Richerche.

References

CAPACCIO, G., GIACOMELLO, P. & GIGLIO, E. (1971). *Acta Cryst.* A**27**, 229–233.

CARRUTHERS, J. R., FEDELI, W., MAZZA, F. & VACIAGO, A. (1973). *J. Chem. Soc.* (*B*), pp. 1558–1563.

COIRO, V. M., GIACOMELLO, P. & GIGLIO, E. (1971). *Acta Cryst.* B**27**, 2112–2119.

COIRO, V. M., GIGLIO, E. & QUAGLIATA, C. (1972). *Acta Cryst.* B**28**, 3601–3605.

CROMER, D. T. & MANN, J. B. (1968). *Acta Cryst.* A**24**, 321–324.

DOMENICANO, A., SPAGNA, R. & VACIAGO, A. (1969). *Atti Accad. Nazl. Lincei Rend. Classe Sci. Fis. Mat. Nat.* **47**, 331–336.

DOSI, C., GIGLIO, E., PAVEL, V. & QUAGLIATA, C. (1973). *Acta Cryst.* A**29**, 644–650.

FEDELI, W., MAZZA, F. & VACIAGO, A. (1970). *J. Chem. Soc.* (*B*), pp. 1218–1223.

GIACOMELLO, P. & GIGLIO, E. (1970). *Acta Cryst.* A**26**, 324–327.

GIGLIO, E. (1969). *Nature, Lond.* **222**, 339–341.

HAMILTON, W. C., ROLLETT, J. S. & SPARKS, R. A. (1965). *Acta Cryst.* **18**, 129–130.

HANSON, H. P., HERMAN, F., LEA, J. D. & SKILLMAN, S. (1964). *Acta Cryst.* **17**, 1040–1044.

JONES, R. A. Y., KATRITZKY, A. R. & MENTE, P. G. (1970). *J. Chem. Soc.* (*B*), pp. 1210–1217.

JONES, R. A. Y., KATRITZKY, A. R., RICHARDS, A. C. & WYATT, R. J. (1970). *J. Chem. Soc.* (*B*), pp. 122–127.

KLYNE, W. & PRELOG, V. (1960). *Experientia*, **16**, 521–523.

STOCKMAYER, W. H. (1941). *J. Chem. Phys.* **9**, 398–402.

Acta Cryst. (1976). B**32**, 885

The Crystal Structure of Calcium 2-Keto-D-gluconate Trihydrate (Calcium D-*arabino*-Hexulosonate Trihydrate)

BY M. A. MAZID AND R. A. PALMER

Department of Crystallography, Birkbeck College, University of London, Malet Street, London WC1E 7HX, England

AND A. A. BALCHIN

Crystallography Laboratory, Department of Applied Physics, Brighton Polytechnic, Moulsecomb, Brighton BN2 4GJ, England

(*Received* 5 *June* 1975; *accepted* 3 *August* 1975)

The crystal structure of calcium 2-keto-D-gluconate (calcium D-*arabino*-hexulosonate) trihydrate, $Ca(C_6H_9O_7)_2.3H_2O$, has been determined by the heavy-atom method and refined by full-matrix least-squares calculations to $R=0{\cdot}094$ for 2235 visually estimated intensities. The crystals are orthorhombic, $P2_12_12_1$, with $a=10{\cdot}438$ (5), $b=18{\cdot}368$ (9), $c=9{\cdot}545$ (4) Å, $Z=4$. Two independent pyran-type rings have formed through lactolization of the ketone groups at C(2) and C(2′). One ring oxygen together with hydroxyl and carboxyl substituents and water of crystallization, provide ninefold coordination for the calcium ions. One 2-ketogluconate ion lies between calcium positions forming chains along the 2_1 axis parallel to **c** through bidentate and tridentate chelate ligands to alternate calcium atoms. An independent 2-ketogluconate ion completes the unusual nine-coordination to calcium through tridentate ligands. The Ca–O distances vary from 2·33 to 2·73 Å with an average value of 2·53 Å.

Introduction

Sequestration of calcium from rocks and soil by 2-ketogluconic acid ($COOH.CO.HOCH.HCOH.HCOH.CH_2OH$) is ascribed to the formation of chelate bonds between the metallic and organic ions.

The effectiveness of 2-ketogluconic acid as a seques-